

Characterisation and reaction to fire of “M5” rigid rod polymer fibres

S. BOURBIGOT, X. FLAMBARD, M. FERREIRA, E. DEVAUX

Laboratoire de Génie et Matériaux Textiles (GEMTEX), UPRES EA2461, Ecole Nationale Supérieure des Arts et Industries Textiles (ENSAIT), BP 30329, 59056 Roubaix Cedex 01, France

E-mail: serge.bourbigot@ensait.fr

F. POUTCH

Centre de Recherche et d'Etude sur les Procédés d'Ignifugation des Matériaux (CREPIM), Parc de la Porte Nord, Rue Christophe Colomb, 62700 Bruay-la-Buissière, France and Laboratoire des Procédés d'Elaboration de Revêtements Fonctionnels (PERF), Ecole Nationale Supérieure de Chimie de Lille, BP 108, 59652 Villeneuve d'Ascq Cedex, France

In this work, the flammability properties of a new rigid rod polymer fibre are examined. This new fibre was called “M5” and is formally poly[2,6-diimidazo[4,5-b:4',5'-e]-pyridinylene-1,4(2,5-dihydroxy)phenylene or PIPD. In a first step, characterisation of PIPD (M5) by solid state NMR confirms the chemical composition of the fibre. The investigation of the fire performance of M5 fibers using the cone calorimeter has shown the excellent behaviour of M5 in comparison with poly-p-phenylenediamine-terephthalamide (PPTA). M5 fibre does not burn even in very severe conditions (flashover conditions). It can then be used where high level of safety is required. The investigation of its heat resistance shows that M5 degrades via exothermic reactions of 30% lower energy than PPTA and have a strong pyrolysis resistance which can explain, in part, its unique fire properties.

© 2003 Kluwer Academic Publishers

1. Introduction

M5 fibres are a new rigid rod polymer with strong hydrogen bonds between polymer chains. M5 is a poly-pyridobisimidazole, formally poly[2,6-diimidazo[4,5-b:4',5'-e]pyridinylene – 1,4(2,5-dihydroxy)phenylene (PIPID and called “M5”) (Fig. 1) [1–7]. It has the ability to form hydrogen bonds between adjacent chains. These hydrogen bonds that can be formed between the polymer chains should result in a higher lateral interaction, thus leading to improved compressive properties [3, 7]. M5 fibre has unique properties and has a great potential for developing materials such as lightweight composites, hard and soft ballistic armour, high strength cables or advanced fabrics and textiles.

Using X-ray diffraction, a structural model for the “as spun” fibre was proposed [2–4]. In the model, planar polymer chains are located at the corners and the centre. The model contains four water molecules for each PIPD molecule, hydrogen bonded in layers that separate layers of polymer chains packed face to face. The crystalline density of the crystal hydrate is 1.6 g/cm³. In order to improve the mechanical properties, PIPD fibres were subjected to a heat treatment under tension. The structural transitions during the heat treatment had been investigated by X-ray diffraction again. The fibre changes from a crystal hydrate into a dehydrated structure in which hydrogen bonds are formed between the polymer chains. The intermolecular hydrogen bonds

form a bi-directional hydrogen bonding network resulting in three dimensional crystalline order. The two dimensional projection cell describing the lateral packing is rectangular and contains two polymer chains located at its centre and corners. The crystalline density of the heat treated PIPD is 1.77 g/cm³.

Solid state nuclear magnetic resonance (NMR) is a powerful tool for characterising and studying the structural and dynamical properties of oriented polymers [8]. Using high resolution solid state NMR, the chemical composition of PIPID can be examined. As far as we know, PIPD has never been characterised by solid state NMR and the purpose of this work is to get further information on PIPD using this technique. In the first part of this study, the chemical composition of PIPD is investigated by cross-polarisation (CP) – magic angle spinning (MAS) – high power dipolar decoupling (DD) NMR ¹³C and by use of the interrupted decoupling experiment for selecting non protonated carbon resonances [9].

It is reported that PIPD (M5) has high fire resistance properties like the other rigid-rod polymeric fibres [10]. It is due to its lack of a true melting point, the rigidity of the chain, and the strong chain-to-chain interaction. PIPD (M5) does not burn in air and is self extinguishing. Its LOI (Limiting Oxygen Index measured according to [11]) is reported to be greater than 50 vol%. It means that PIPD has a great potentiality for flame retardancy.

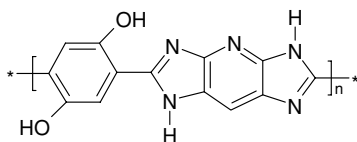


Figure 1 Repetition unit of PIPD (M5).

Generally, fibres with LOI greater than 25 vol% are said to be flame retardant. Nevertheless, LOI test is not very representative of a fire even if it allows to rate quantitatively the materials. The approach that we have developed is to evaluate fibres using the cone calorimeter as a fire model [12, 13]. The major advantage of the cone calorimeter is to measure the rate of heat release which is the quantity of most concern in predicting the course of the fire and its effect [14]. The second part of this work examines the reaction of fire of M5 as a knitted fabric using the cone calorimeter as a fire model. It is completed by studying the heat resistance of M5 fibres. Indeed, the fire behaviour of a material depends on processes occurring in both condensed and gas phase and on the processes of heat and mass transfer. These processes strongly depend on the degradation reactions occurring in the condensed phase [15].

2. Experimental

2.1. Materials

Poly(2,6-diimidazo[4,5-b:4',5'-e]pyridinylene-1,4(2,5-dihydroxy)phenylene) (PIPD or M5) fibres were supplied as multifilament (92 Tex) by Magellan (USA) (hot drawn yarn). Poly-p-phenylenediamine-terephthalamide fibres (PPTA) fibres as multifilament (90 Tex) are classical Kevlar[®]29.

2.2. High resolution ¹³C NMR

¹³C NMR measurements were performed on a Bruker ASX100 operated at 25.2 MHz (2.35 T) with magic angle spinning (MAS), high power ¹H decoupling (DD) and ¹H-¹³C cross polarization (CP) using a 7 mm probe. The Hartmann-Hahn matching condition was obtained by adjusting the power on ¹H channel for a maximum ¹³C FID (free induction decay) signal of adamantane. Spectra were acquired with contact times of 1 ms. A repetition time of 10 s was used for all samples. The reference used was tetramethylsilane and the spinning speed was 5000 Hz. The values of chemical shift are verified using adamantane and adamantanone before starting a new experiment. For these products, the chemical shifts were within ±0.2 ppm.

Interrupted decoupling experiment was carried out by gating off the decoupler before the ¹³C FID acquisition time. The decoupler was turned on again during the acquisition period. The delay between the last 180° ¹³C pulse and acquisition time allows the dephasing delay to vary from 0 to 120 μs. The delay is long enough to suppress the signals from carbons with attached protons.

2.3. Processing

Fabrics have been made by knitting different yarns on an automatic rectilinear machine gauge 7. The struc-

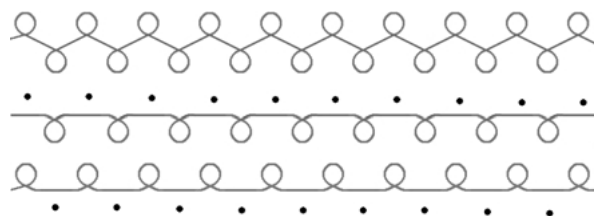


Figure 2 Double woven rib knitted structure.

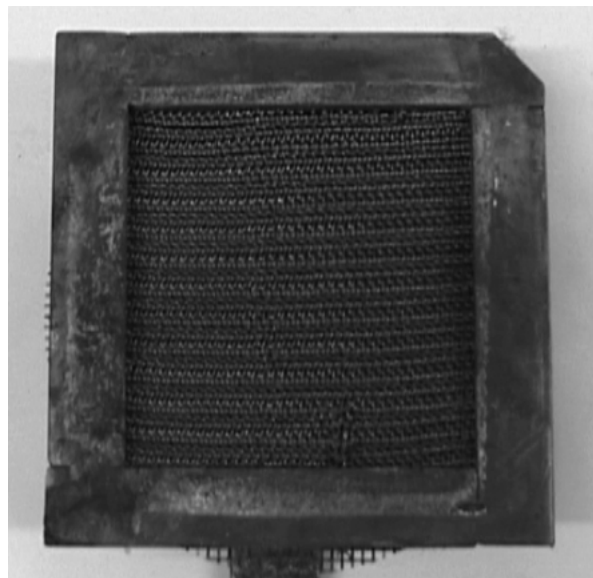


Figure 3 Knitted M5 fibres in a home made cone calorimeter holder used in the experiments.

ture used is a woven rib (Fig. 2). The samples have the surface weight equalling 1.08 ± 0.05 kg/m².

2.4. Cone calorimetry by oxygen consumption

Samples were exposed to a Stanton Redcroft Cone Calorimeter at an external heat flux of 75 kW/m². This flux corresponds to flashover conditions [12, 13]. The samples are mounted between two cut steel sheets placed on the usual holder of the cone calorimeter (Fig. 3). The surface exposed to the external heat flux is 9 × 9 cm². Our method does not correspond to any standard. Conventional cone calorimetry data (Rate of Heat Release (RHR), Total Heat Evolved (THE) by integrating RHR curve versus time, Volume of Smoke Production (VSP) (see the computation in [14]) and Fire Growth Rate Index (FIGRA) (see the computation in [16]) were obtained using a software developed in our laboratory. The experiments were repeated 3 times. When measured at 75 kW/m² external heat flux, RHR and VSP values are reproducible to within ±10% and CO, CO₂ were reproducible to within ±15%. The results presented in the following section are averages. The cone data reported in this work are the average of three replicated experiments.

2.5. Thermal analysis

Simultaneous TGA/DSC measurements were performed using a Netzsch STA 449C Jupiter apparatus

under air flow (50 mL/min) at 10°C/min from 20°C to 1200°C. Samples (about 5 mg) were placed in Pt crucibles with a cap on the top (the cap had a hole in the centre). The calibration in temperature and in energy was made using standards: biphenyl, KClO₄, K₂CrO₄, BaCO₃ and benzoic acid.

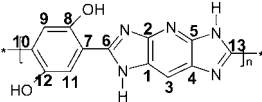
3. Results and discussion

3.1. NMR characterisation

CP-DD-MAS ¹³C NMR spectrum of M5 is shown in Fig. 4. Three bands at 150, 130, 115 ppm can be distinguished on the spectrum which correspond to different magnetically non equivalent carbons.

The DD techniques rely on a fundamental principle that in absence of ¹H decoupling field, the ¹³C magnetization will diphase or decay as a result of ¹H-¹³C dipolar interaction. The rate of dephasing of the ¹³C signal is related to the magnitude of dipolar interaction which depends on geometrical factors [9]. Therefore, in the DD spectrum with long dephasing delay, the resonances observed are mainly of non-protonated and weakly coupled carbons. Fig. 5 shows ¹³C NMR spectra of M5 versus dephasing delay. It can be seen that the intensity of the band at 115 ppm decreases versus dephasing delay till 40 μs. The other bands seem to be unchanged even at very long dephasing delay (>100 μs). This result suggests that the carbons at 115 ppm are protonated carbons and that the others are nonprotonated carbons. According to the literature [17–20] and to the experiment of Fig. 5, the different carbons can be assigned. 160–100 ppm is the zone corresponding to the aromatic and polyaromatic compounds. This is in agreement with the repeat unit of M5. The assignments of carbons are given Table I. As noticed above,

TABLE I Assignments of bands of PIPD NMR spectrum

Repeat unit of PIPD (M5)	Bands (ppm)
	(3), (7), (9), (10) and (11) – 115 ppm
	(1), (4) and (5) – 130 ppm
	(2), (6), (8), (12) and (13) – 150 ppm

the band at 115 ppm corresponds to protonated and non-protonated carbons. It explains therefore why the band decreases but it is not totally removed (Table I).

3.2. Reaction to fire

Fire hazard is associated with a variety of properties of a material in a particular scenario. It is determined by a combination of factors including the material ignitability, the rate at which heat is released from it when it burns, the total amount of heat that is released, the flame spread, the smoke production and the toxicity of the smoke. It has now been established that the property which most critically defines a fire is the heat release, because two conditions are necessary for propagating a fire from the ignited material to another one and/or to the surroundings. First, sufficient energy, as heat, needs to be released to cause secondary ignition. Secondly, the heat release needs to be occurred sufficiently fast so that the heat is not quenched in the “cold” air. By using heat release equipment, as the cone calorimeter, the different parameters discussed above can be measured in the same instrument, in a manner generally relevant to real fires.

To evaluate our samples, fibres were knitted as fabric because we assume that it is more significant than samples as staple or as yarns, even if the textile structure

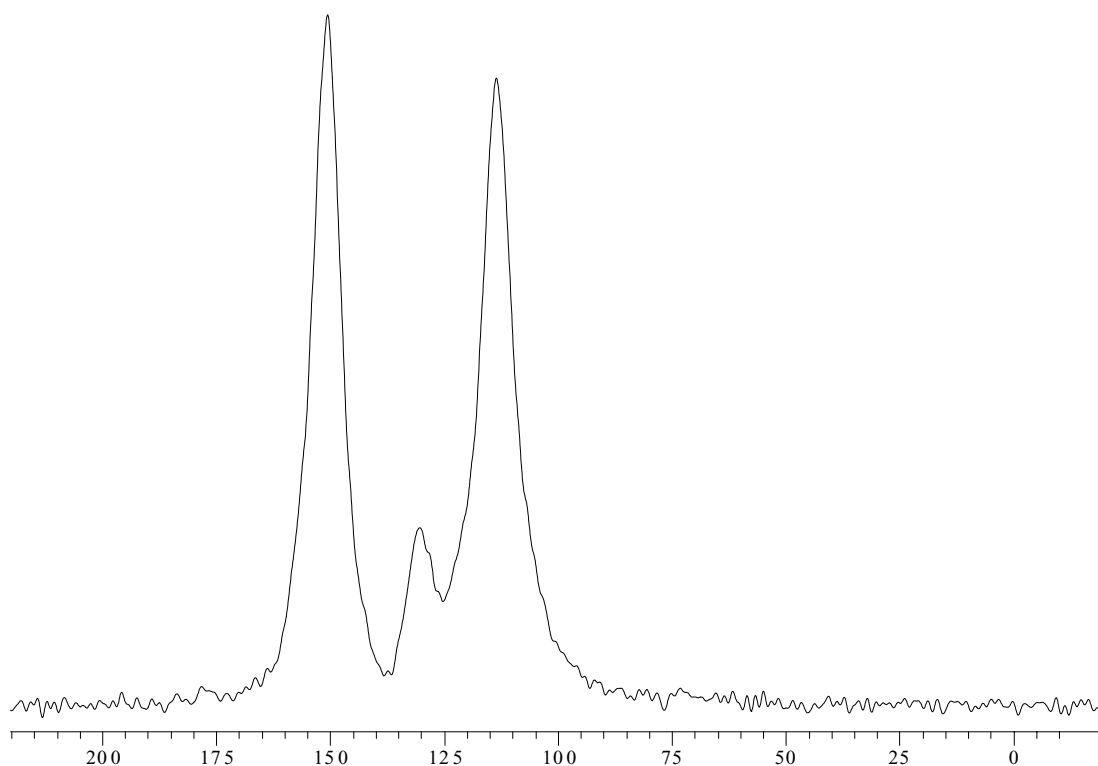


Figure 4 CP-DD-MAS NMR ¹³C of “M5” fibre.

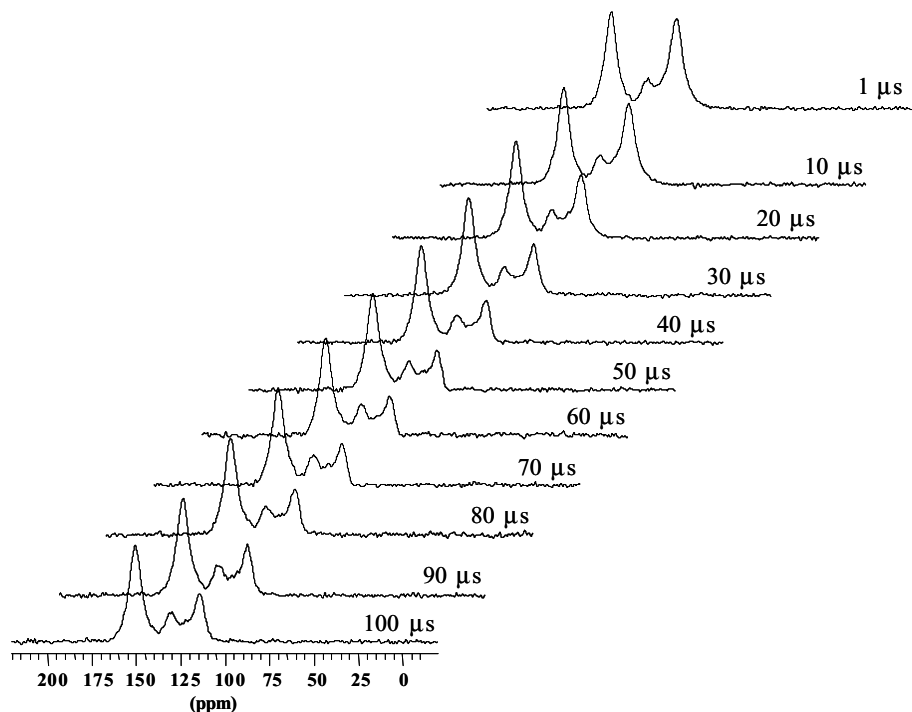


Figure 5 CP-DD-MAS NMR ^{13}C spectra of PIPD (M5) fibre versus dephasing delay.

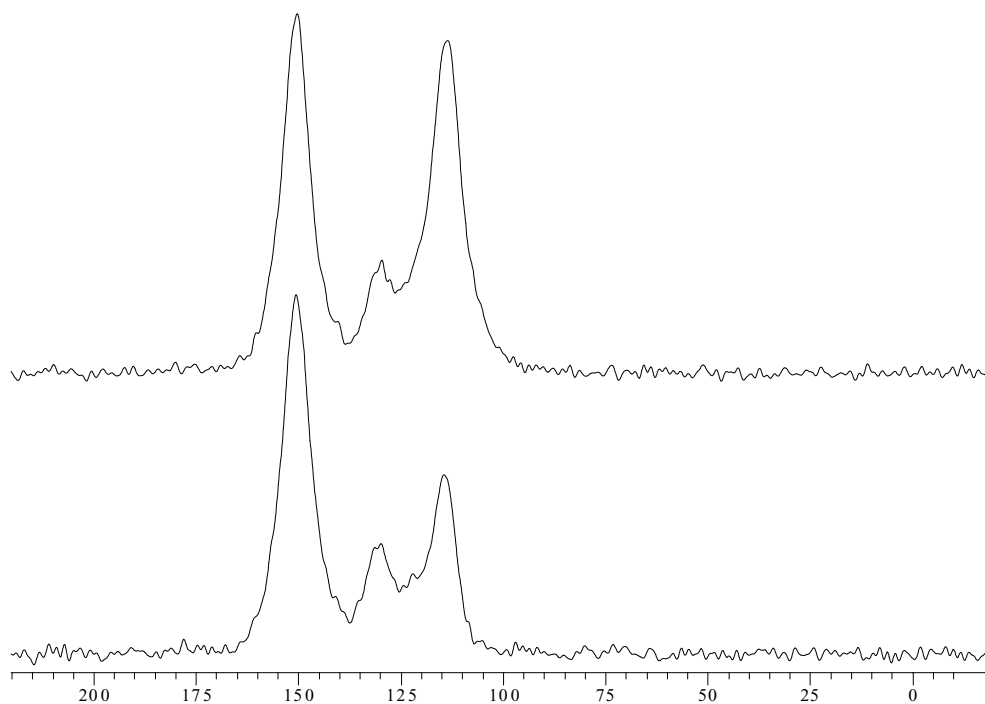


Figure 6 CP-DD-MAS NMR ^{13}C spectra of PIPD (M5) fibre with (down) and without (up) dephasing delay.

may play a role in the reaction to fire of the fabric [21]. RHR curves of knitted PPTA, and PIPD fibres should present a superior behaviour in comparison with PPTA. RHR peak of PIPD is only 50 kW/m^2 in comparison with 300 kW/m^2 for PPTA fibres demonstrating that PIPD has a very high fire resistance even in very severe conditions (an external heat flux of 75 kW/m^2 can be considered as flashover conditions) (Fig. 7).

Visual observation confirms the RHR results. It can be seen on Fig. 8 that PPTA burns with high flames whereas PIPD only glows with very small flames.

THE curves (Fig. 9) show the values of PIPD are strongly reduced in comparison with that ones of PPTA. THE of PPTA increases strongly at the beginning of the combustion. THE of PIPD increases comparatively slowly. During fire, the storage of heat will be high for PPTA fabrics and low for PIPD.

FIGRA (Fire Growth Rate Index) is a good indicator of the contribution to fire growth of a material. FIGRA curves of PPTA and PIPD fibres are shown in Fig. 10. FIGRA curves of M5 show only one peak at 80 s (FIGRA = 50 W/s). In the case of PPTA, two peaks are observed at 10 s (FIGRA = 190 W/s) and at 60 s

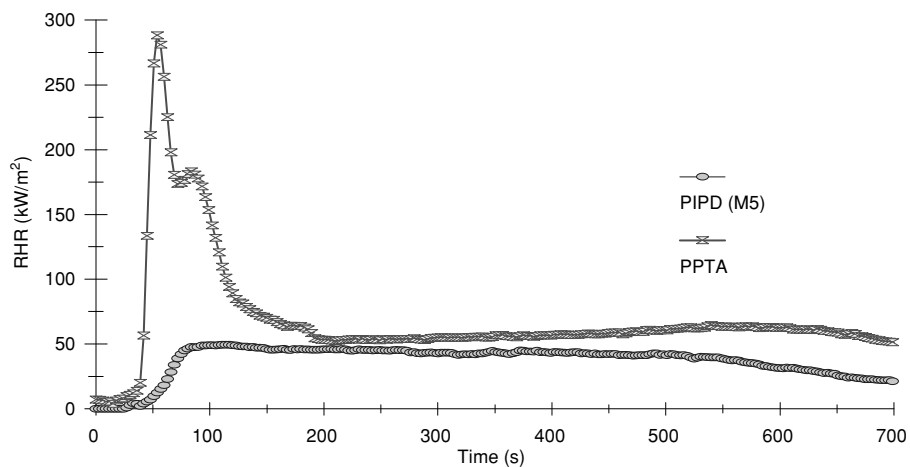


Figure 7 RHR curves of knitted PPTA and PIPD (M5) fibers.

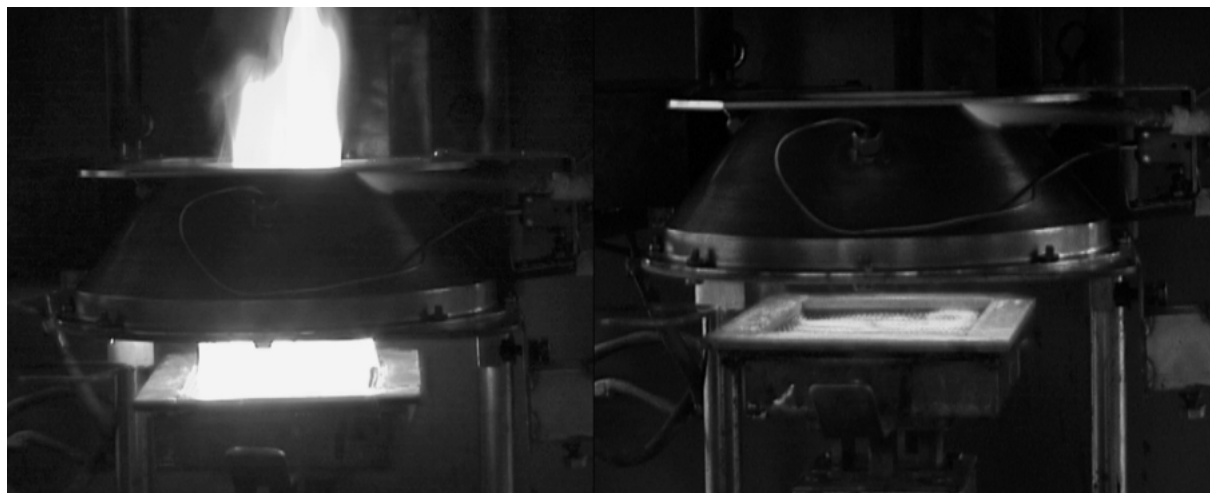


Figure 8 Fire behaviour of PPTA (left) and PIPD (M5) (right).

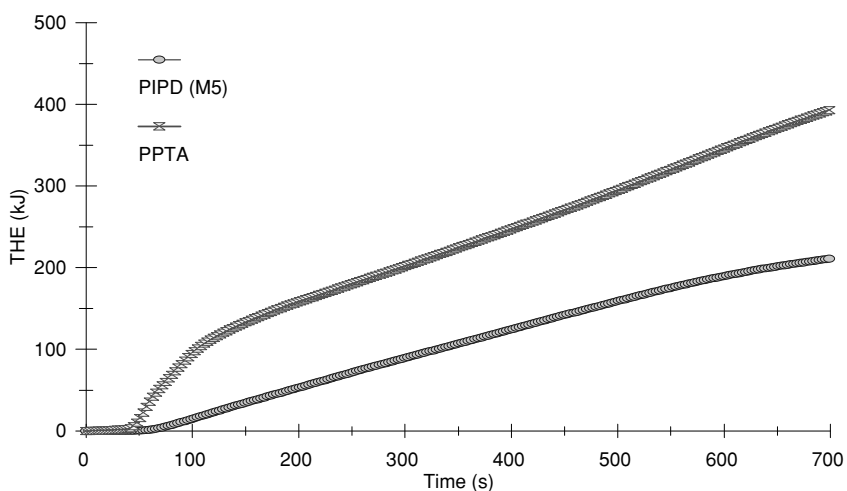


Figure 9 THE curves of knitted PPTA and PIPD (M5) fibres.

(FIGRA = 450 W/s). The contribution of fire growth of PIPD is therefore comparatively very low. It means that the contribution to fire growth of PPTA is fast.

Smoke obscuration is strongly lowered using M5 in comparison with PPTA (Fig. 11). PPTA fibres evolve smoke in a double peak at 0.006 m³/s (~50 s) and

0.0035 m³/s (~75 s). M5 does not contribute to the smoke obscuration during fire whereas the smoke production of burning PPTA is comparatively high. It is very important in term of safety of people because the obscuration of a room or a corridor leads generally to a large panic effect. Indeed panic gives rise to more deaths than the fire itself.

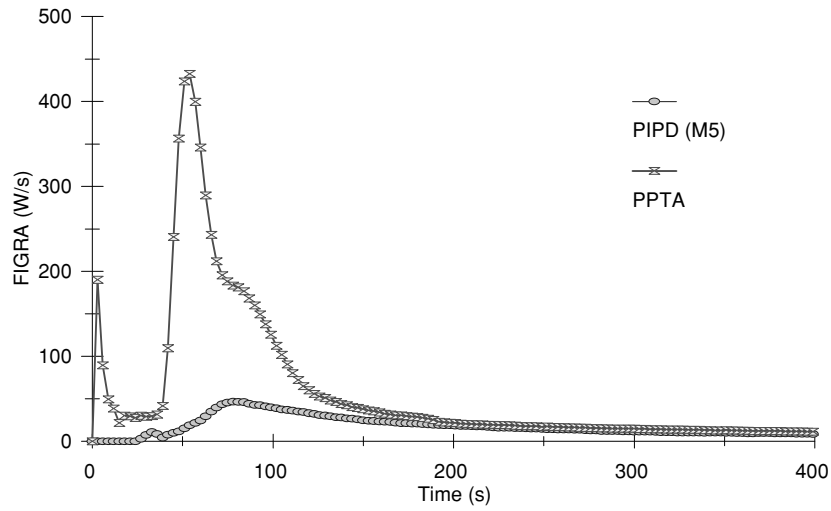


Figure 10 FIGRA curves of knitted PPTA and PIPD (M5) fibres.

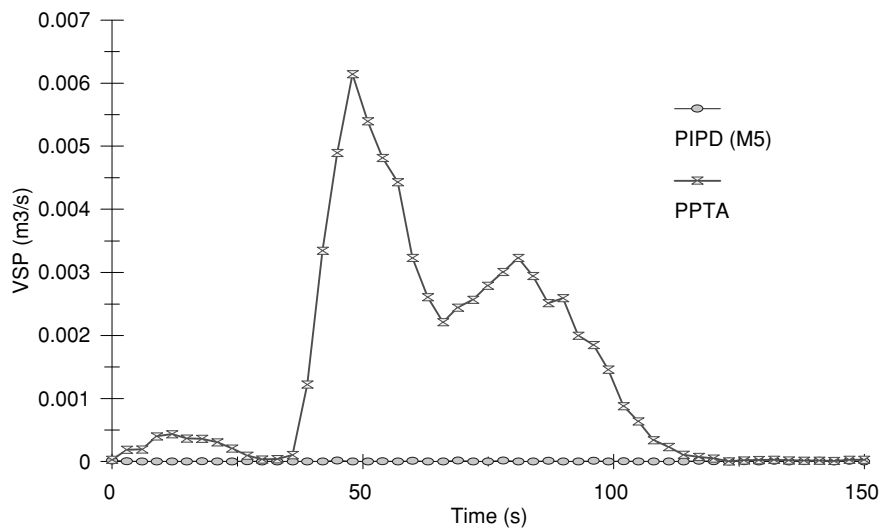


Figure 11 VSP curves of knitted PPTA and PIPD (M5) fibres.

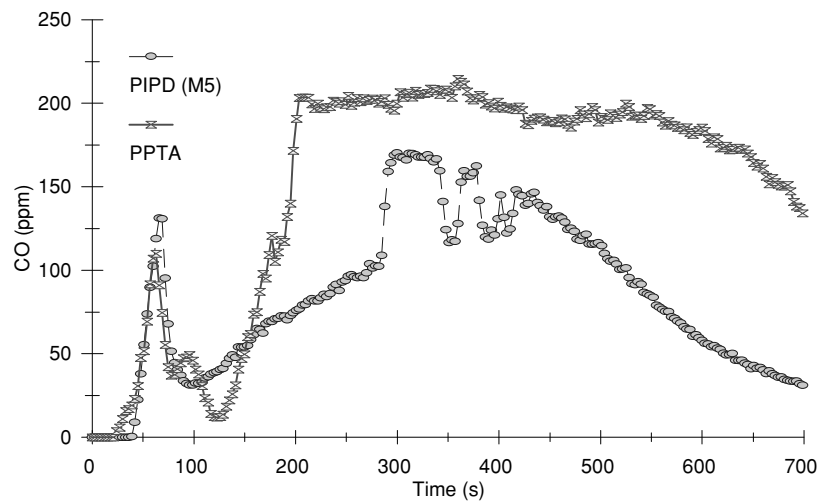


Figure 12 CO curves of knitted PPTA and PIPD (M5) fibres.

Fig. 12 presents the CO production versus time evolved in the experimental conditions of the cone calorimeter, close to the conditions of ventilated room. PIPD and PPTA exhibit sharp peaks at 35 s (CO peaks = 125 ppm). Then, CO production of PPTA increases again and reaches a plateau at about 200 ppm. From

600 s, it decreases to zero. Meanwhile, CO production of PIPD is chaotic about a mean value equalling 125 ppm. It decreases from 450 s to zero.

The curves of CO₂ amounts evolved by the fibres are similar to the RHR curves (Fig. 13). The same conclusions can be given. PPTA evolves

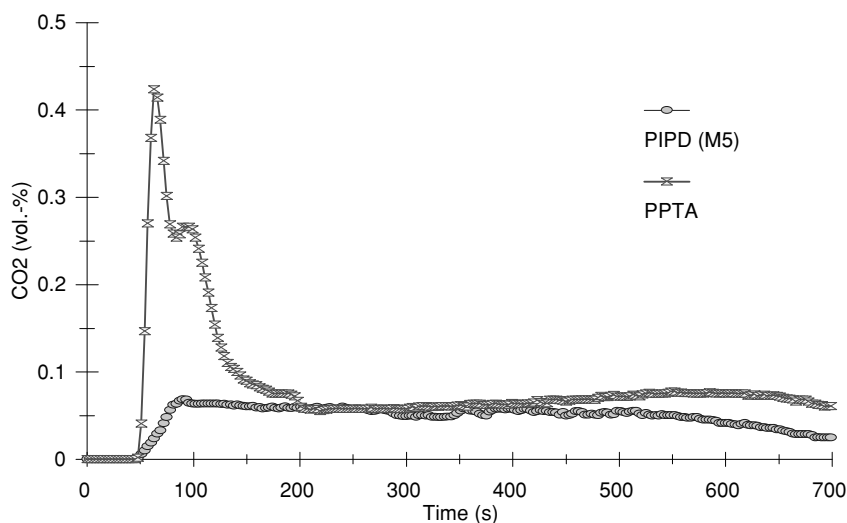


Figure 13 CO₂ curves of knitted PPTA and PIPD (M5) fibres.

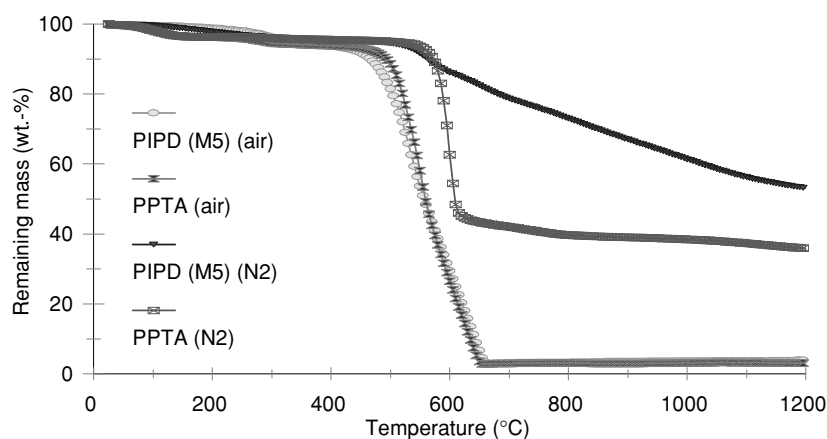


Figure 14 TG curves of PIPD (M5) vs. PPTA under air flow or nitrogen flow (heating rate = 10°C/min; air flow).

comparatively high amount of CO₂ in comparison with PIPD.

3.3. Heat resistance

TG curves of the thermo-oxidative and pyrolytic degradations of PPTA and PIPD fibres show the strong influence of the oxygen (Fig. 14). The thermo-oxidative degradation of PIPD fibres is similar to PPTA but in pyrolytic conditions, PIPD exhibits much higher thermal stability than PPTA. The main degradation of PIPD and PPTA in thermo-oxidative conditions occurs between 450 and 650°C. The final residues at 1200°C are about 4 wt%. In pyrolytic conditions, the degradations of the two fibres are shifted towards higher temperatures (from 450°C to 600°C). PPTA degrades much faster than PIPD and forms a stable residue of 40 wt%. PIPD degrades comparatively slowly from 450°C to 1200°C and the residue formed at 1200°C is 55 wt%. This last consideration is important when it is recalled that the burning process depends on the thermal degradation reactions in the condensed phase, which generate volatile products and, that the polymeric substrate heated by an external source is pyrolysed with the generation of combustible fuel in a zone where there is depletion of oxygen [23].

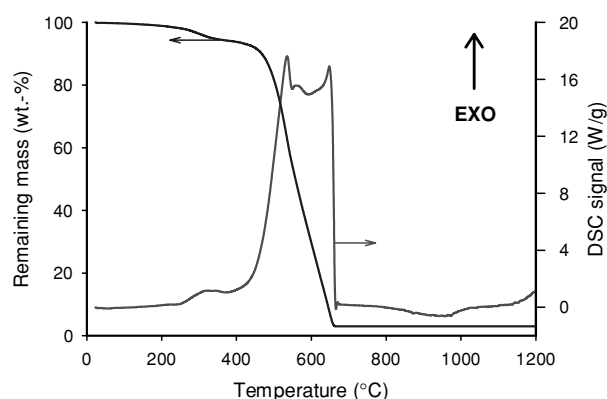


Figure 15 Simultaneous TG/DSC curves of PIPD (M5) fibre (heating rate = 10°C/min; air flow).

Simultaneous TG/DSC experiments on the two fibres show that the degradation of the fibres is associated to high exothermal decomposition (Fig. 15 shows the TG/DSC curves of PIPD as typical example). The thermo-oxidative decompositions of the fibres are exothermic which can be assigned to oxidation reactions.

It is shown that the enthalpy of decomposition of PIPD fibres is decreased by 30% in comparison with

TABLE II Enthalpy of decomposition of PPTA and PIPD (M5) fibres

Fibre	Enthalpy of decomposition (J/g)	Temperature range of computation (°C)
PPTA	-23500	400-700
PIPD (M5)	-17000	400-700

PPTA (Table II). In addition of the better thermal stability of PIPD in pyrolytic conditions, this result could explain the better fire behaviour of PIPD in regard to PPTA because in the conditions of fire, it can be expected that the degradation reactions of M5 are less exothermic than PPTA ones. It is to note that these values are in the same order of magnitude as the heat of combustion of common organic polymers as well [22]. In particular, the heat of combustion of PPTA is measured to be -26 kJ/g [22] and it is close to that measured in Table II by simultaneous TGA/DSC. This last consideration confirms therefore our assumption. Finally, it can be proposed that the unique flammability properties of PIPD are the combination of at least two effects: a strong pyrolysis resistance and a comparatively low enthalpy of decomposition.

4. Conclusion

Solid state NMR characterisation of PIPD (M5) has confirmed the chemical composition of the fibre. The investigation of the fire performance of PIPD fibres using the cone calorimeter has shown the excellent behaviour of PIPD in comparison with PPTA. PIPD fibre does not burn even in very severe conditions (flashover conditions). It can then be used where high level of safety is required. The investigation of its heat resistance shows that PIPD degrades via exothermic reactions of 30% lower energy than PPTA and has a strong pyrolysis resistance which can be explained, in part, its unique fire properties.

Acknowledgement

The Authors thanks Prof. Sikkema from Magellan Systems International for helpful discussion on PIPD (M5) fibre and for supplying M5 fibres. They are indebted to Mr. Dubusse from CREPIM for his skilful experimental assistance in cone calorimeter, and to Mrs. Sabine Chlebicki from GEMTEX for her skilful experimental assistance in TGA/DSC experiments. Mr. Bertrand

Revel from Centre Commun de Mesures RMN is acknowledged for helpful discussion and experimental assistance in NMR experiments.

References

1. D. SIKKEMA, *Polymer* **39**(24) (1998) 5981.
2. M. LAMMERS, PhD thesis, Swiss Federal Institute of Technology Zurich, 1998.
3. E. A. KLOP and M. LAMMERS, *Polymer* **39**(24) (1998) 5987.
4. M. LAMMERS, E. A. KLOP, M. G. NORTHOLT and D. SIKKEMA, *ibid.* **39**(24) (1998) 5999.
5. JAGT VAN DER and A. BEUKERS, *ibid.* **40** (1999) 1035.
6. J. C. L. HAGEMAN, J. W. VAN DER HORST and R. A. DE GROOT, *ibid.* **40** (1999) 1313.
7. J. SIRICHAISIT and R. J. YOUNG, *ibid.* **40** (1999) 3421.
8. In "NMR Spectroscopy of Polymers," edited by R. N. Ibbett (Pub. Blackie Academic & Professional an Imprint of Chapman & Hall, London, 1993).
9. S. J. OPELLA and M. H. FREY, *J. Amer. Chem. Soc.* **101** (1979) 5854.
10. <http://www.m5fiber.com>.
11. Limiting Oxygen Index, "Standard Test Method for Measuring Minimum Oxygen Concentration to Support Candle-Like Combustion of Plastics," ASTM D 2863.
12. V. BABRAUSKAS, in "Development of Cone Calorimeter—A Bench Scale Rate of Heat Release Based on Oxygen Consumption," *NBS-IR 82-2611*, US Nat. Bur. Stand., Gaithersburg, 1982.
13. *Idem.*, *Fire and Mater.* **8**(2) (1984) 81.
14. V. BABRAUSKAS and S. J. GRAYSON, in "Heat Release in Fires" (Pub. Elsevier Science Publishers Ltd., London, England, 1992).
15. Y. P. KHANNA, E. M. PEARCE, B. D. FORMAN and D. A. BINI, *Polym. Sci.: Polym. Chem. Ed.* **19** (1981) 2799.
16. CEN/TC127N 1424, "Reaction to Fire Tests on Building Products ("SBI" test)," Draft 26 February 1999.
17. W. L. EARL and D. L. VANDERHART, *J. Magn. Reson.* **48** (1982) 35.
18. G. E. MACIEL, V. J. BARTUSKA and F. P. MIKNIS, *Fuel* **58** (1979) 391.
19. S. BOURBIGOT, M. LE BRAS, R. DELOBEL, R. DESCRESSAIN and J. P. AMOUREUX, *J. Chem. Soc.-Faraday Trans.* **92**(1) (1996) 149.
20. T. M. DUNCAN and D. C. DOUGLASS, *J. Chem. Phys.* **87** (1984) 339.
21. S. BOURBIGOT and X. FLAMBARD, in "Fire and Materials: Flammability of Textiles," edited by A. R. Horrocks and S. Bourbigot (Pub. Wiley Interscience, 2002) vol. 26, p. 153.
22. R. N. WALTERS, S. M. HACKETT and R. E. LYON, *Fire and Mater.* **24** (2000) 245.
23. M. LEWIN, in "Fire Retardancy of Polymers: The Use of Intumescent," edited by M. Le Bras, G. Camino, S. Bourbigot and R. Delobel (Pub. Royal Chem. Soc., Cambridge, 1998) p. 3.

Received 25 July

and accepted 12 November 2002